protein level but also influenced by another mechanism in the nigrostriatal projection.

In this study, we showed that (i) the TH protein expression was abrogated in a subset of dopaminergic neurons (AAV-Cre-infected neurons); (ii) the striatal dopamine contents were better maintained than the TH protein levels; and (iii) *in vivo* L-DOPA synthesis activity per TH protein level was enhanced. Because L-DOPA synthesis activity was virtually retained in only the TH-expressing axons, these results suggest that L-DOPA synthesis activity per TH protein in a given axon is partly affected by dopamine synthesis in the neighboring axons. Such trans-axonal regulation of dopamine synthesis activity might be a basis for the homeostasis of dopaminergic transmission in the striatum.

Consistent with our data, in a rat model of preclinical parkinsonism where nigrostriatal dopaminergic neurons were lesioned by 6-OHDA, TH activity was increased relative to dopamine loss (35). In such models generated with 6-OHDA, however, it is difficult to know if the enhanced TH activity observed after 6-OHDA administration is a result of a direct toxic effect of 6-OHDA on the remaining axons, a cell death of neighboring axons, or a decrease in tissue dopamine level. In contrast, our genetic manipulation specifically targets the *Th* gene in AAV-Cre-infected neurons, so our results demonstrate the effect of *Th* gene deletion on TH protein levels, dopamine contents, and L-DOPA synthesis activity more clearly and simply.

It remains to be determined how trans-axonal compensation of dopamine is mediated. For example, TH homospecific activity may be changed for the compensation by phosphorylation. D2 autoreceptors on dopaminergic axon terminals may be involved in controlling the dopamine level (36). However, it is not clear whether D2 autoreceptors modify dopamine synthesis in the long term. For example, chronic administration of haloperidol, a D2 receptor inhibitor, does not increase the basal levels of Ser(P)-31-TH and Ser(P)-40-TH in mice (37). We could not detect significant change in the Ser(P)-31-TH and Ser(P)-40-TH levels.

TH is also controlled by a feedback inhibition loop by dopamine (27). For example, a decrease in extracellular dopamine level by *Th* gene ablation may cause lower dopamine reuptake (38), lower local dopamine concentration in axon terminals, and a relief of TH from the feedback inhibition. Previous reports suggest that the concentration of released dopamine can be on the order of micromolar and is quickly taken up by DAT into dopaminergic axons (38). Because intracellular dopamine concentration is probably <100 nM (39), local intracellular dopamine concentration could be affected by dopamine reuptake. Meanwhile, TH has two dopamine-binding sites: high affinity (K_d < 4 nM) and low affinity (K_d = 90 nM) (40). Therefore, most TH proteins would be the dopamine-bound form for the high affinity site, whereas the low affinity site may be more relevant to feedback inhibition by dopamine (40).

Alternatively, there is a circuit level feedback (8) or neurotrophic factors, such as glial cell-derived neurotrophic factor (41). Further studies will be required to clarify the signaling mechanisms underlying the trans-axonal regulation of dopamine levels.

We found that the ratio of DOPAC and HVA contents to dopamine did not change, whereas, in Parkinson disease patients and model animals, DOPAC/DA and HVA/DA ratios were reported to be increased (7, 10, 42). This difference may exist because in our experimental conditions, most of the dopaminergic axons were preserved after the *Th* gene ablation, and those axons may have participated in the reuptake of extracellular dopamine, resulting in minimal effects on the dopamine degradation rate.

Adjusting Dopamine Storage for Compensation—If the number of dopamine-synthesizing axons was decreased by more than half, where and how were dopamine molecules stored for compensation? Because we did not observe any gross changes in the vMAT2 and DAT protein levels, it is unlikely that the numbers of dopaminergic synaptic vesicles and terminals were drastically changed. Otherwise, vesicular dopamine contents may be increased in the remaining TH-expressing axons for the compensation. For example, treatment of cultured dopaminergic neurons with L-DOPA or glial cell-derived neurotrophic factor increased vesicular dopamine levels more than 3-fold (41). Alternatively, it is also possible that the low level dopamine was contained in the TH-negative axons through the reuptake of spilled-over dopamine from neighboring synapses. This mechanism is consistent with the idea that released dopamine is spilled over and taken up by neighboring axons (38). Thus, the compensation of dopamine levels in our experimental system may accompany an increase in vesicular dopamine contents and/or spill-over and reuptake of released dopamine by TH-negative axons.

Taken together, in this study, we develop a conditional gene targeting method to efficiently and selectively inactivate the *Th* gene in the SNc dopaminergic neurons in adult mice without inducing neuronal degeneration. The analysis of these mutant mice revealed that TH protein levels in the axon terminals are regulated differently from the level in the soma, and the tissue dopamine levels are under trans-axonal compensatory regulation, where the reduction of dopamine in some axons induces up-regulation of dopamine synthesis activity in other axons. We believe that the present findings represent at least one of the compensatory mechanisms in Parkinson disease and are related to actions of remedies for psychiatric disorders.

Acknowledgments—We are most grateful to Professor Pierre Chambon for supporting this project. We thank Jean-Marc Bornert and the Institut de Génétique et de Biologie Moléculaire et Cellulaire/Institut Clinique de la Souris embryonic stem and mouse facility for excellent technical assistance. We thank Naomi Takino and Hiroko Nishida for technical assistance in constructing the AAV vectors. We thank Felix Schlegel for technical assistance with immunohistochemistry. We thank Dr. Pavel Osten for kindly providing the Synapsin I promoter construct.

REFERENCES

1. Graybiel, A. M., Canales, J. J., and Capper-Loup, C. (2000) *Trends Neurosci.* **23,** S71–S77
2. Schultz, W. (2007) *Trends Neurosci.* **30,** 203–210
3. Fahn, S. (2003) *Ann. N.Y. Acad. Sci.* **991,** 1–14
4. Grace, A. A., Floresco, S. B., Goto, Y., and Lodge, D. J. (2007) *Trends*

Neurosci. **30,** 220–227
5. Tye, K. M., Tye, L. D., Cone, J. J., Hekkelman, E. F., Janak, P. H., and Bonci, A. (2010) *Nat. Neurosci.* **13,** 475–481
6. Simpson, E. H., Kellendonk, C., Kandel, E. (2010) *Neuron* **65,** 585–596
7. Bernheimer, H., Birkmayer, W., Hornykiewicz, O., Jellinger, K., Seitelberger, F. (1973) *J. Neurol. Sci.* **20,** 415–455
8. Bezard, E., Gross, C. E., and Brotchie, J. M. (2003) *Trends Neurosci.* **26,** 215–221
9. McCallum, S. E., Parameswaran, N., Perez, X. A., Bao, S., McIntosh, J. M., Grady, S. R., and Quik, M. (2006) *J. Neurochem.* **96,** 960–972
10. Pifl, C., and Hornykiewicz, O. (2006) *Neurochem. Int.* **49,** 519–524
11. Perez, X. A., Parameswaran, N., Huang, L. Z., O'Leary, K. T., and Quik, M. (2008) *J. Neurochem.* **105,** 1861–1872
12. Kobayashi, K., Morita, S., Sawada, H., Mizuguchi, T., Yamada, K., Nagatsu, I., Hata, T., Watanabe, Y., Fujita, K., and Nagatsu, T. (1995) *J. Biol. Chem.* **270,** 27235–27243
13. Thomas, S. A., Matsumoto, A. M., and Palmiter, R. D. (1995) *Nature* **374,** 643–646
14. Zhou, Q. Y., Quaife, C. J., Palmiter, R. D. (1995) *Nature* **374,** 640–643
15. Zhou, Q. Y., and Palmiter, R. D. (1995) *Cell* **83,** 1197–1209
16. Szczypka, M. S., Kwok, K., Brot, M. D., Marck, B. T., Matsumoto, A. M., Donahue, B. A., and Palmiter, R. D. (2001) *Neuron* **30,** 819–828
17. Hnasko, T. S., Perez, F. A., Scouras, A. D., Stoll, E. A., Gale, S. D., Luquet, S., Phillips, P. E, Kremer, E. J., and Palmiter, R. D. (2006) *Proc. Natl. Acad. Sci. U.S.A.* **103,** 8858–8863
18. Nagatsu, T., Levitt, M., and Udenfriend, S. (1964) *J. Biol. Chem.* **239,** 2910–2917
19. Li, X. G., Okada, T., Kodera, M., Nara, Y., Takino, N., Muramatsu, C., Ikeguchi, K., Urano, F., Ichinose, H., Metzger, D., Chambon, P., Nakano, I., Ozawa, K., and Muramatsu, S. (2006) *Mol. Ther.* **13,** 160–166
20. Kadkhodaei, B., Ito, T., Joodmardi, E., Mattsson, B., Rouillard, C., Carta, M., Muramatsu, S., Sumi-Ichinose, C., Nomura, T., Metzger, D., Chambon, P., Lindqvist, E., Larsson, N. G., Olson, L., Björklund, A., Ichinose, H., and Perlmann, T. (2009) *J. Neurosci.* **16,** 15923–15932
21. Dittgen, T., Nimmerjahn, A., Komai, S., Licznerski, P., Waters, J., Margrie, T. W., Helmchen, F., Denk, W., Brecht, M., and Osten, P. (2004) *Proc. Natl. Acad. Sci. U.S.A.* **101,** 18206–18211
22. Paxinos, G., and Franklin, K. B. (2004) *The Mouse Brain in Stereotaxic Coordinates,* Academic Press, Inc., San Diego, CA
23. Prensa, L., and Parent, A. (2001) *J. Neurosci.* **21,** 7247–7260
24. Matsuda, W., Furuta, T., Nakamura, K. C., Hioki, H., Fujiyama, F., Arai, R., and Kaneko, T. (2009) *J. Neurosci.* **29,** 444–453
25. Ungerstedt, U., and Arbuthnott, G. W. (1970) *Brain Res.* **24,** 485–493
26. Lane, E. L., Cheetham, S., and Jenner, P. (2005) *J. Pharmacol. Exp. Ther.* **312,** 1124–1131
27. Dunkley, P. R., Bobrovskaya, L., Graham, M. E., von Nagy-Felsobuki, E. I., and Dickson, P. W. (2004) *J. Neurochem.* **91,** 1025–1043
28. Tank, A. W., Curella, P., and Ham, L. (1986) *Mol. Pharmacol.* **30,** 497–503
29. Fernández, E., and Craviso, G. L. (1999) *J. Neurochem.* **73,** 169–178
30. Lin, A. C., and Holt, C. E. (2008) *Curr. Opin. Neurobiol.* **18,** 60–68
31. Willis, D. E., and Twiss, J. L. (2006) *Curr. Opin. Neurobiol.* **16,** 111–118
32. Jarrott, B., and Geffen, L. B. (1972) *Proc. Natl. Acad. Sci. U.S.A.* **69,** 3440–3442
33. Terada, S. (2003) *Neurosci. Res.* **47,** 367–372
34. Hirokawa, N., Niwa, S., and Tanaka, Y. (2010) *Neuron* **68,** 610–638
35. Zigmond, M. J., Acheson, A. L., Stachowiak, M. K., and Stricker, E. M. (1984) *Arch. Neurol.* **41,** 856–861
36. Cubeddu, L. X., and Hoffmann, I. S. (1982) *J. Pharmacol. Exp. Ther.* **223,** 497–501
37. Håkansson, K., Pozzi, L., Usiello, A., Haycock, J., Borrelli, E., and Fisone, G. (2004) *Eur. J. Neurosci.* **20,** 1108–1112
38. Rice, M. E., and Cragg, S. J. (2008) *Brain Res. Rev.* **58,** 303–313
39. Mosharov, E. V., Larsen, K. E., Kanter, E., Phillips, K. A., Wilson, K., Schmitz, Y., Krantz, D. E., Kobayashi, K., Edwards, R. H., and Sulzer, D. (2009) *Neuron* **62,** 218–229
40. Gordon, S. L., Quinsey, N. S., Dunkley, P. R., and Dickson, P. W. (2008) *J. Neurochem.* **106,** 1614–1623
41. Pothos, E. N., Davila, V., and Sulzer, D. (1998) *J. Neurosci.* **18,** 4106–4118
42. Hefti, F., Enz, A., and Melamed, E. (1985) *Neuropharmacology* **24,** 19–23
43. Fukushima, T., and Nixon, J. C. (1980) Anal. Biochem. **102,** 176–188

Supplemental Figure Legends

Supplemental Fig. 1 Linearity in the quantification of TH proteins by Western blot.
Serial dilutions of striatal homogenates were prepared from the uninjected side of three mice and subjected to Western blot for TH. The linearity in the relationship between loaded protein level and detected TH signals was evaluated. Black, gray, and open circles represent data sets from individual mice. We employed a range showing linear relationship between actual loaded protein (2.5 to 20 μg, or 0.125 to 1.0 in ratios) and measured TH protein level (0.05 to 1 in ratio). The black line indicates a linear fitting. Dashed line has a slope of one.

Supplemental Fig. 2
A, Summarized quantitative analyses of Western blots for the striatal AADC protein levels. N = 8, 9, 13 and 5 brains for 2, 4, 8 weeks ($Th^{fl/fl}$ mice) and 8 weeks ($Th^{+/+}$ mice) after injection, respectively.
B, The relationship between rotation behavior and dopamine contents. 16 weeks after AAV-Cre injection, the mice were administered with DAT inhibitor, GBR12909 (30 mg/kg, i.p.), and ipsilateral rotation in 60 min was counted. One week later, striatal dopamine contents were measured. The dopamine content and ipsilateral rotation behavior showed significantly negative correlation (Spearman's rank correlation, $p = 0.0350$, $\rho = -0.94$). Gray line shows an exponential curve fitting.

Supplemental Fig.3 The relationship between dopamine and dopamine metabolites.
A, The relationship between HVA and dopamine contents in the $Th^{fl/fl}$ mice 8 weeks after the AAV-Cre injection. The data indicate the ratio of the HVA contents in the AAV-Cre injected side of the striatum normalized to the uninjected side. The open circles indicate individual data. The dotted line has a slope of one, and the solid line indicates a linear fitting. N = 13 mice. Spearman's rank correlation, $p = 0.0008$, $\rho = 0.97$ for HVA vs. dopamine.
B, Summarized ratios of the DOPAC and HVA to dopamine in the $TH^{fl/fl}$ mice 8 weeks after the AAV-Cre injection. (U) and (I) indicate the uninjected and injected sides of the striatum, respectively. Data indicate mean ± s.e.m..

Supplemental Fig. 4 Western blot analysis of the phospho-TH proteins.
A, pSer40-TH and pSer31-TH levels were examined by Western blot using antibodies against total, pSer40-, and pSer31-TH. Homogenates were prepared 8 weeks after the AAV-Cre injection.
B, *C*, Summary of scattered plots of pSer40-TH (*B*) and pSer31-TH (*C*) against total TH protein levels. Dotted lines have a slope of one. The protein levels of pSer40-TH and pSer31-TH are correlated to the total TH protein level in the $Th^{fl/fl}$ mice (Spearman's rank correlation, $p = 0.0054$, $\rho = 0.98$ for pSer40-TH vs. total TH; $p = 0.0063$, $\rho = 0.97$ for pSer31-TH vs. total TH). N = 6, 3 for $Th^{fl/fl}$ and $Th^{+/+}$, respectively. Note that there was no trend toward an increase in the ratio of phospho-TH to total TH protein level when total TH protein level was decreased.

Supplemental Fig. 5 Lack of changes in the striatal vMAT2 and DAT protein levels.
A, Representative Western blot for vMAT2 and DAT. Western blot was performed using crude synaptosomal fractions from the striatum of $Th^{fl/fl}$ mice prepared 8 weeks after AAV-Cre injection. The TH and β-actin protein levels were also examined. (U) and (I) indicate uninjected and injected side of the striatum, respectively. Note that while the TH protein level was reduced in the injected side, vMAT2 and DAT proteins did not show a reduction.
B, Summary of the quantification of Western blot data for vMAT2, DAT, and TH in the $Th^{fl/fl}$ and $Th^{+/+}$ mice. The ratios of protein levels in the injected side to the uninjected side are shown. The open circles indicate the values from individual animals, and the bars indicate the means. n

= 7, 3 for the $Th^{fl/fl}$ and $Th^{+/+}$, respectively. p = 0.31, 0.91, and 0.0167 for vMAT2, DAT, and TH, respectively, Mann-Whitney U test.

C, *D*, Relationship of protein levels between vMAT2 and TH proteins (*C*) or DAT and TH protein (*D*) were examined by scattered plots. The lines indicate linear fitting. There was no significant correlation (p = 0.42, 0.60 for vMAT2 vs. TH and DAT vs. TH, respectively, Spearman's rank correlation test).

Supplemental Fig. 1

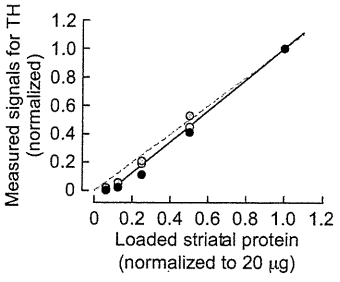

Supplemental Fig. 2

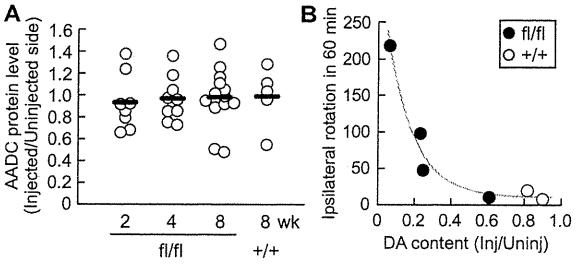

Supplemental Fig. 3

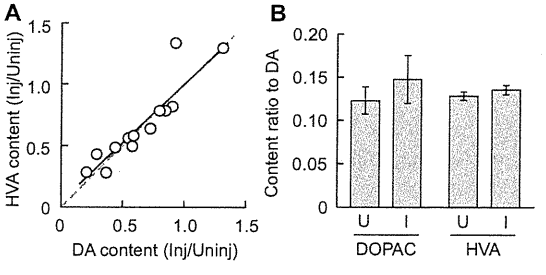

Supplemental Fig. 4

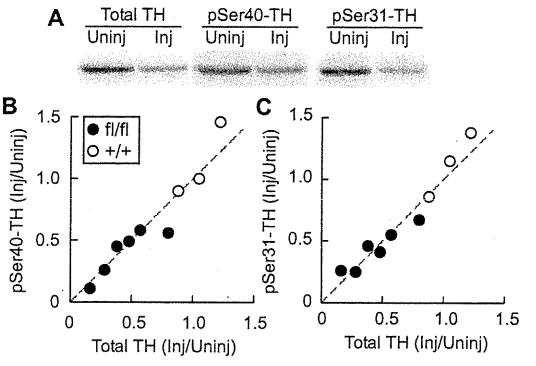

Supplemental Fig. 5

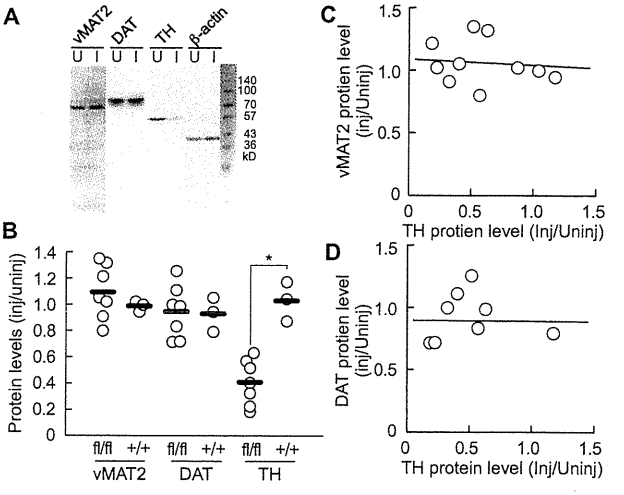

RESEARCH ARTICLE

Cortically Evoked Responses of Human Pallidal Neurons Recorded During Stereotactic Neurosurgery

Hiroki Nishibayashi, MD,[1]* Mitsuhiro Ogura, MD, PhD,[1] Koji Kakishita, MD, PhD,[1] Satoshi Tanaka, MD,[1] Yoshihisa Tachibana, DDS, PhD,[2] Atsushi Nambu, MD, PhD,[2] Hitoshi Kita, PhD,[3] and Toru Itakura, MD, PhD[1]

[1]*Department of Neurological Surgery, Wakayama Medical University, Wakayama, Japan*
[2]*Division of System Neurophysiology, National Institute for Physiological Sciences and Department of Physiological Sciences, The Graduate University for Advanced Studies, Okazaki, Japan*
[3]*Department of Anatomy and Neurobiology, College of Medicine, University of Tennessee Memphis, Memphis, USA*

ABSTRACT: Responses of neurons in the globus pallidus (GP) to cortical stimulation were recorded for the first time in humans. We performed microelectrode recordings of GP neurons in 10 Parkinson's disease (PD) patients and 1 cervical dystonia (CD) patient during surgeries to implant bilateral deep brain stimulation electrodes in the GP. To identify the motor territories in the external (GPe) and internal (GPi) segments of the GP, unitary responses evoked by stimulation of the primary motor cortex were observed by constructing peristimulus time histograms. Neurons in the motor territories of the GPe and GPi responded to cortical stimulation. Response patterns observed in the PD patients were combinations of an early excitation, an inhibition, and a late excitation. In addition, in the CD patient, a long-lasting inhibition was prominent, suggesting increased activity along the cortico-striato-GPe/GPi pathways. The firing rates of GPe and GPi neurons in the CD patient were lower than those in the PD patients. Many GPe and GPi neurons of the PD and CD patients showed burst or oscillatory burst activity. Effective cathodal contacts tended to be located close to the responding neurons. Such unitary responses induced by cortical stimulation may be of use to target motor territories of the GP for stereotactic functional neurosurgery. Future findings utilizing this method may give us new insights into understanding the pathophysiology of movement disorders. © 2011 *Movement* Disorder Society

Key Words: globus pallidus; microelectrode recording; cortical stimulation; stereotactic functional neurosurgery; Parkinson's disease; dystonia

Introduction

Deep brain stimulation (DBS) is a well-established treatment for advanced movement disorders, such as Parkinson's disease (PD).[1,2] Major targets of DBS are the globus pallidus (GP) and the subthalamic nucleus (STN). Although there is a trend toward targeting more at the STN, GP-DBS has several advantages, including amelioration of drug-induced dyskinesia and fewer adverse neuropsychological effects.[3] GP-DBS is also efficient to treat severe generalized or segmental dystonia.[4] The optimal target of GP-DBS is the posteroventral part of the internal segment of the GP (GPi), corresponding to its motor territory.[3,5–7] To identify the motor territory of the GPi, microelectrode recordings (MERs) of neuronal activity, such as spontaneous firing patterns and responses to passive and active movements, have been performed.[4,8,9]

Studies in nonhuman primates have shown that stimulation of the motor cortices can identify somatotopically organized motor territories in the external segment of the GP (GPe) and GPi.[10–13] In this study, we tested whether a similar method can be used to identify motor territories in the human GP. We recorded responses of GP neurons induced by motor cortical stimulation during stereotactic neurosurgery

Additional Supporting Information may be found in the online version of this article.

* **Correspondence to:** Hiroki Nishibayashi, Department of Neurological Surgery, Wakayama Medical University, 811-1 Kimiidera, Wakayama, 641-0012, Japan; hirokin@wakayama-med.ac.jp

Relevant conflict of interest/financial disclosures: Nothing to report. This study was supported by Wakayama Foundation for the Promotion of Medicine to T.I., Grants-in-Aid for Scientific Research (B) (18300135) from the Ministry of Education, Culture, Sports, Science and Technology of Japan and the Uehara Memorial Foundation to A.N., and NIH grants NS-47085 and NS-57236 to H. K.
Full financial disclosures and author roles may be found in the online version of this article.

Received: 26 April 2010; **Revised:** 1 September 2010; **Accepted:** 3 October 2010
Published online 10 February 2011 in Wiley Online Library (wileyonlinelibrary.com). DOI: 10.1002/mds.23502

of PD and cervical dystonia (CD) patients and compared them with responses of nonhuman primates. These data will also provide clues to understanding the pathophysiology of movement disorders.

Patients and Methods

Patients

This study was approved by the ethical committee of Wakayama Medical University and has followed its guidelines. The operations were performed on 10 PD patients and 1 CD patient (Supporting Information Table 1). The 8 male and 2 female PD patients were of mean age 61.9 years (range 50–72), had a mean disease duration of 126 months (48–168), and a mean levodopa dosage of 460 mg/day (300–800). Preoperative unified Parkinson's disease rating scale (UPDRS) was a mean best score of 25.3 (0–53) and a mean worst score of 66.6 (41–93). The 62-year-old female CD patient had a disease duration of 32 months and a Toronto western spasmodic torticollis rating scale (TWSTRS) score of 54. All patients received bilateral GP-DBS electrode implantation.

Surgical Procedure and MERs

Medications were withdrawn 18 hours before operation in most patients (Supporting Information Table 1). Surgery including MERs was performed without general anesthesia in most cases. Propofol was injected intravenously (2 mL/kg/hr) if necessary (patients 2, 5, and 11). Burr holes were made bilaterally on the coronal suture about 30 mm lateral from the midline. After dural incision, a strip electrode with four platinum discs (diameter of 5 mm) spaced 10 mm apart (UZN C1-04-04-10-1-A, Unique Medical; Tokyo, Japan) was inserted into the subdural space in the posterolateral direction and placed on the upper limb area of the primary motor cortex (MI). To avoid injury to the cortical veins, special care was taken during insertion of the strip electrode and no complications were noted. Electrical stimuli (1–20 mA strength, 1.0 ms duration monophasic constant current pulse at 1 Hz) were delivered through two of the four discs. A pair of discs inducing muscle twitches in the contralateral upper limb at the lowest intensity was selected and the motor threshold (T) was determined. In the following recordings, stimuli were delivered through this pair at the intensity inducing clear muscle twitches ($1.2–1.5 \times T$) at 1 Hz. A microelectrode (FC1002, Medtronic; Minneapolis, MN) was inserted through the same burr hole targeting the tentative target in the posteroventral GPi (20 mm lateral to the midline, 4 mm ventral to the intercommissural line, and 3 mm anterior to the midcommissural point), which was determined based on the magnetic resonance imaging (MRI). Neuronal activity was amplified, displayed (Leadpoint 9033A0315, Medtronic), and fed to a computer for on-line analysis. The responses induced by MI-stimulation were assessed by constructing peristimulus time histograms (PSTHs; bin width of 1 ms) for 20–120 stimulus trials using the software (LabVIEW 7.1, National Instruments; Austin, TX). Neuronal activity was also stored on a digital audio tape (DAT) recorder (PC204Ax, SONY; Tokyo, Japan) for off-line analysis. Somatosensory responses to joint manipulations and muscle palpations of the upper limb, lower limb, and orofacial regions were also examined. We performed only one or two recording electrode penetrations in each hemisphere because this was a trial study. The GPe/GPi border (the medial medullary lamina) and the ventral border of the GPi were identified by absence of unitary activity. Based on the MERs mappings, DBS electrodes (Model 3387, Medtronic) were implanted bilaterally into the same track of MERs. The deepest electrode contact was positioned within the GPi close to the ventral border. Pulse generators were later implanted bilaterally in the chest. Monopolar (the pulse generator was used as an anode) or bipolar stimulation was applied, and the most effective contacts of DBS electrodes to improve clinical symptoms were determined. Postoperative MRI verified the position of DBS electrodes in the posteroventral GPi, and the recording sites were estimated.

Off-line Data Analysis

Neuronal activity was played back from DAT, isolated by a window discriminator, converted into digital data, and fed to a computer. Responses induced by MI-stimulation were assessed by constructing PSTHs. The mean values and standard deviations of the firing rate during 100 ms preceding the stimulation onset were calculated from PSTHs and were considered to be the values for base discharge. Responses to MI-stimulation were judged to be significant if the firing rate during at least two consecutive bins (2 ms) reached the statistical level of $P < 0.05$ (one-tailed t-test). The latency of the response was defined as the time at which the firing rate first exceeded this level. Mean firing rates and patterns were analyzed from autocorrelograms (bin width, 0.5 ms) constructed from 50 s of digitized recordings. Spontaneous firing pattern was assessed by visual inspection of the autocorrelograms: Burst activity was inferred from the existence of a single peak, and oscillatory burst activity was inferred from multiple peaks and troughs.

Results

Neuronal activity was recorded at 163 sites along 27 electrode tracks in 21 hemispheres of 11 patients (Supporting Information Table 1). Single unit activity was isolated at 157 sites, and activity of 147 neurons (59 GPe and 88 GPi) was recorded long enough to

TABLE 1. Response patterns of GPe and GPi neurons evoked by cortical stimulation and numbers of oscillatory burst neurons recorded from the PD and CD patients

	GPe			GPi		
	Cortical stimulation			Cortical stimulation		
Patient	No. of responsive neurons/no. of neurons recorded	Response patterns and no. of neurons	No. of oscillatory burst neurons	No. of responsive neurons/no. of neurons recorded	Response patterns and no. of neurons	No. of oscillatory burst neurons
PD						
1	0/0		0	0/2		1
2	1/6	1 inh	2	2/6, (5/5)	2 inh, (1 inh+ex, 4 inh)	0, (2)
3	0/1		0	0/4		0
4	4/7	1 inh, 3 late ex	0	0/12		0
5	0/0, (0/2)		0	0/0		0
6	1/2	1 inh	1	1/4	1 ex+inh+ex	2
7	0/2		0	0/5		1
8	2/2	1 ex+inh+ex, 1 inh+ex	0	2/4	1 ex+inh, 1 late ex	3
9	4/10	4 inh	1	7/17	1 ex+inh, 1 inh+ex, 1 early ex, 1 inh, 3 late ex	0
10	6/15	1 ex+inh+ex, 3 inh+ex, 1 early ex, 1 inh	1	9/14	2 ex+inh+ex, 1 ex+inh, 2 inh+ex, 3 inh, 1 late ex	2
PD total	18/45, (0/2)	2 ex+inh+ex, 4 inh+ex, 1 early ex, 8 inh, 3 late ex	5	21/68, (5/5)	3 ex+inh+ex, 3 ex+inh, 3 inh+ex, 1 early ex, 6 inh, 5 late ex, (1 inh+ex, 4 inh)	9, (2)
CD						
11	4/11, (0/1)	1 ex+inh, 1 inh+ex, 1 inh, 1 late ex	6	6/13, (1/2)	2 ex+inh, 4 inh, (1 late ex)	1, (2)
Total	22/56, (0/3)		11	27/81, (6/7)		10, (4)

Numbers in parentheses, recorded under propofol
CD, cervical dystonia; ex, excitation; GPe and GPi external and internal segments of the globus pallidus; inh, inhibition; PD, Parkinson's disease.

construct PSTHs from at least 20 stimulus trials (mean of 43) (Table 1). Among them, 137 neurons (56 GPe and 81 GPi) were recorded without general anesthesia and used for further studies. The upper limb area of the MI was successfully identified in all hemispheres tested, and the stimulus intensity of 4–16 mA was used (Supporting Information Table 1).

Responses Evoked by MI-Stimulation

Among 137 neurons, MI-stimulation induced responses in 49 neurons (36%; 22/56 in GPe, 27/81 in GPi) (Table 1). In the PD patients, response patterns to MI-stimulation were combinations of an early excitation, an inhibition, and a late excitation (Fig. 1, A1–A4). A monophasic inhibition (Fig. 1, A1) was the major response pattern (36%; 8/18 in GPe, 6/21 in GPi). Other response patterns were also observed (Table 1): a biphasic response consisting of an inhibition and a subsequent excitation (Fig. 1, A2; 18%) or an excitation and a subsequent inhibition (8%); a triphasic response consisting of an early excitation, an inhibition and a late excitation (Fig. 1, A3 and A4; 13%); and a monophasic early (5%) or late (20%) excitation. On the other hand, in the CD patient, a long-lasting monophasic inhibition (Fig. 1, A5; 50%) and a long-lasting inhibition preceded by an excitation (Fig. 1, A6; 30%) were the typical response patterns (Table 1).

The latency and duration of each component are compared in Table 2. The durations of the inhibitions in the GPe and GPi of the CD patient were significantly longer than those of the PD patients, respectively (t-test, $P < 0.05$). The latency of the inhibition in the GPi of the CD patient was significantly longer than that of the PD patients (t-test, $P < 0.01$).

Spontaneous Activity

Among 137 neurons, spontaneous activity of 71 neurons (28 GPe and 43 GPi) was recorded long enough for analysis. The mean firing rates of GPe and GPi neurons in the PD patients were significantly higher than those of GPe and GPi neurons in the CD patient, respectively (Table 2; t-test, $P < 0.05$). Besides 71 neurons, activity of six neurons was recorded under propofol administration and had a tendency to decreased activity.

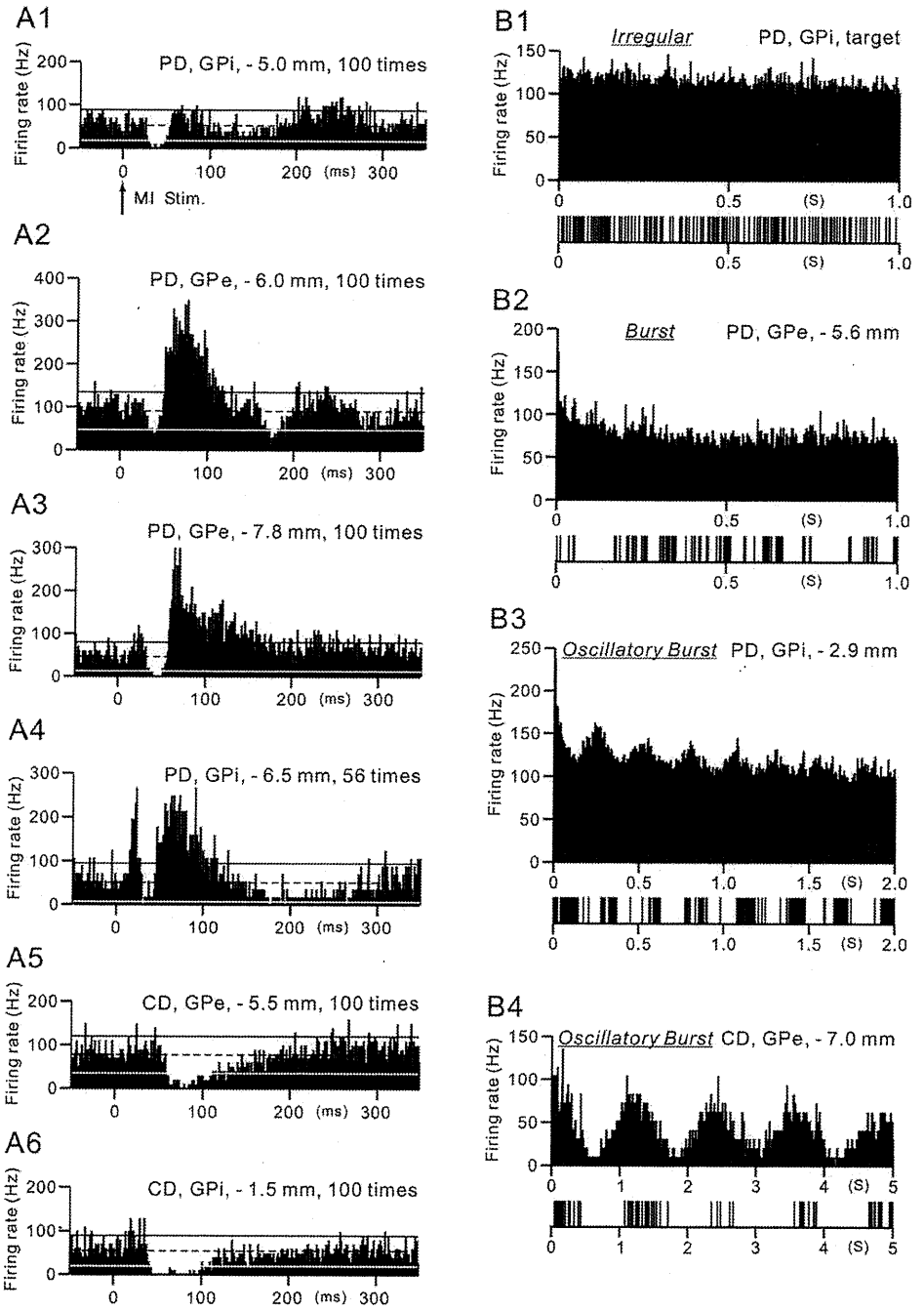

FIG. 1. A: Peristimulus time histograms (PSTHs; bin width of 1 ms) showing the responses of neurons in the external (GPe) and internal (GPi) segments of the globus pallidus evoked by stimulation of the upper limb area of the primary motor cortex in the Parkinson's disease (PD) (A1–A4) and cervical dystonia (CD) (A5 and A6) patients. Cortical stimulation was given at time = 0 (arrow in A1). Recorded sites indicated by the distance from the tentative target (negative distance, above the target) and the numbers of stimulus trials were also shown. The mean firing rate and the statistical levels of $P < 0.05$ (one-tailed *t*-test) calculated from the firing rate during 100 ms preceding the onset of stimulation are indicated by black dotted lines (mean), a black solid line (upper limit of $P < 0.05$), and a white solid line (lower limit of $P < 0.05$), respectively. **B**: Autocorrelograms and slow traces of digitized spikes of GPe and GPi neurons recorded from the PD (B1–B3) and CD (B4) patients. Neuronal activity can be classified into irregular, burst, and oscillatory burst types.

Based on the slow traces of digitized spikes and autocorrelograms, spontaneous firing patterns could be classified into three types: irregular, burst, and oscillatory burst (Fig. 1, B). Irregular neurons fired randomly and were characterized by the flat autocorrelogram (Fig. 1, B1). Burst neurons showed grouped discharges and a single peak around time 0 in the autocorrelogram (Fig. 1, B2). Oscillatory burst neurons showed repetitive grouped discharges and multiple cycles of peaks and troughs in the

TABLE 2. Latencies and durations of cortically evoked responses and spontaneous firing rates in GPe and GPi neurons of the PD and CD patients

	PD		CD	
	GPe	GPi	GPe	GPi
Latency (mean ± SD, ms)				
Early excitation	22.3 ± 5.0 (n = 3)	22.5 ± 8.8 (n = 7)	22.0 (n = 1)	22.0 ± 4.2 (n = 2)
Inhibition	32.6 ± 11.1(n = 14)	34.2 ± 9.9[a] (n = 15)	46.0 ± 4.6 (n = 3)	48.7 ± 7.9[a] (n = 6)
Late excitation	60.7 ± 14.4 (n = 9)	56.2 ± 14.3 (n = 11)	79.0 ± 31.1(n = 2)	(-)
Duration (mean ± SD, ms)				
Early excitation	6.3 ± 7.5 (n = 3)	5.8 ± 4.4 (n = 7)	16.0 (n = 1)	2.5 ± 0.71 (n = 2)
Inhibition	16.1 ± 7.4[b] (n = 14)	19.1 ± 12.2[c] (n = 15)	42.3 ± 34.6[b] (n = 3)	37.5 ± 15.6[c] (n = 6)
Late excitation	27.6 ± 33.7 (n = 9)	25.7 ± 39.2 (n = 11)	2.5 ± 0.71 (n = 2)	(-)
Spontaneous firing rate	81.0 ± 52.5[d] (n = 17)	92.7 ± 40.1[e] (n = 34)	45.8 ± 17.6[d] (n = 11)	62.3 ± 12.1[e] (n = 9)
(mean ± SD, Hz)	[-]	[47.2 ± 23.6 (n = 3)]	[46.7 (n = 1)]	[27.1 ± 36.7 (n = 2)]

Values in brackets, recorded under propofol.
[a]$P < 0.01$.
[b,c,d,e]$P < 0.05$, significantly different from each other (t-test).

autocorrelogram (Fig. 1, B3 and B4). Most neurons [94% (16/17) in GPe and 68% (23/34) in GPi in PD, 100% (11/11) in GPe and 78% (7/9) in GPi in CD] showed burst or oscillatory burst activity (Table 3). In the PD patients, more GPe neurons showed burst or oscillatory burst activity than GPi neurons ($P < 0.05$, Fisher's exact test). Oscillatory frequency of oscillatory burst neurons in the PD patients was mostly in the delta (1–4 Hz) or theta–alpha (4–12 Hz) band, while that in the CD patient was mostly in the delta band.

Locations of Recorded Neurons

Locations of recorded neurons are plotted in Figure 2. GPe/GPi neurons responding to MI-stimulation were found in clusters along electrode tracks, although the rostral and the lateral part of the GPe were not explored. Among 49 GPe/GPi neurons responding to MI-stimulation, 12 neurons (24%) responded to passive movements of the upper limb, such as shoulder, elbow, wrist, or digits. On the other hand, among 43 GPe/GPi neurons responding to passive movements of the upper limb, 12 neurons (28%) responded to MI-stimulation. Neurons responding to passive movements of the lower limb were found in the different area from the upper limb area. Neurons responding to jaw movements were mainly found in the ventral to middle part of the GPi.

Correlation between Clinical Benefits and Neuronal Responses

Monopolar (14 sides) or bipolar (eight sides) electrical stimulation (1.5–3.5 V constant voltage, 210 μs duration, at 185 Hz) was applied for DBS. The most effective cathodal contacts were located in the dorsal (11 sites), middle (two sites), ventral (six sites) GPi, or ventral GPe (three sites; Fig. 2, Supporting Information Table 2). For the PD patients, symptoms were assessed using UPDRS III and IV (items 18–35) before and 10–20 days after starting DBS (Supporting Information Table 2). Symptoms were ameliorated in all patients, and the DBS was markedly effective (score ≥ 10) in four patients (patients 2, 6, 8, and 10) and fairly effective (score ≥ 5) in other four patients (patients 3, 4, 7, and 9). Noticeably improved symptoms (score ≥ 4) were rigidity (patients 2, 3, 7, 8, and 10), bradykinesia (patients 2, 6, 8, and 10), tremor (patients 4, 6, and 8), and dyskinesia (patient 10). In the CD patient, the TWSTRS score decreased from 54 to 34, and unilateral cervical rotation was markedly improved. The most effective cathodal contacts tended to be located close to the responding neurons (Fig. 2).

Discussion

Responses Evoked by MI-Stimulation

In this study, the responses of GPe/GPi neurons induced by MI-stimulation were composed of various combinations of an early excitation, an inhibition, and a late excitation in human subjects. In the GPe, GPi and substantia nigra pars reticulata (SNr) of monkeys

TABLE 3. Spontaneous firing patterns of GPe and GPi neurons recorded from the PD and CD patients

	PD		CD	
Spontaneous firing pattern	GPe	GPi	GPe	GPi
Irregular	1	11	0	2
Burst	11	14	5	6
Oscillatory burst	5	9	6	1
<4 Hz	3	3	6	1
4–12 Hz	2	5	0	0
12 Hz<	0	1	0	0
Total	17	34	11	9

Numbers of GPe and GPi neurons exhibiting irregular, burst, or oscillatory burst activity are shown.

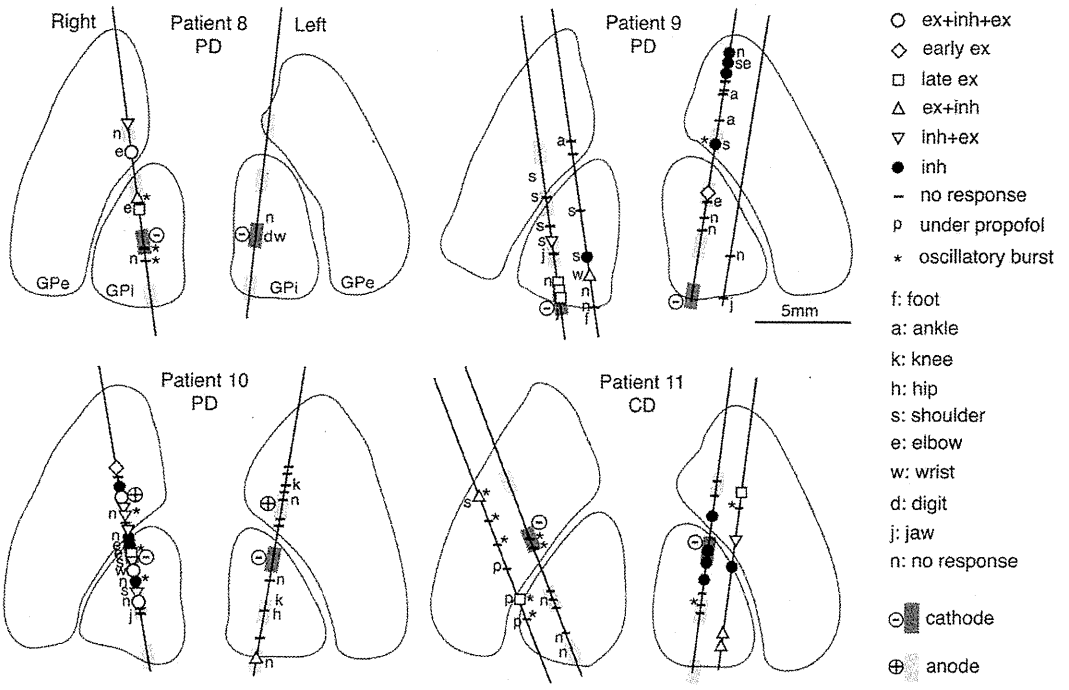

FIG. 2. Locations of recorded neurons in the GPe and GPi of the PD (patients 8, 9, and 10) and CD (patient 11) patients shown in coronal views. Response patterns evoked by cortical stimulation and somatosensory inputs examined by passive manipulations were represented by different symbols. Locations of DBS electrodes were also shown by shaded rectangles (dark rectangle with minus sign, the most effective cathode; light rectangle with plus sign, anode used). In patients 8, 9, and 11, monopolar stimulation was performed using the pulse generator as an anode.

and rodents, cortical stimulation evoked typically a triphasic response, composed of an early excitation, an inhibition, and a late excitation,[10–16] which is very similar to the triphasic response observed in this study (Fig. 1, A3 and A4). Studies in nonhuman primates have clarified that the early excitation is derived from the cortico-STN-GPe/GPi pathway,[10] the inhibition by the cortico-striato-GPe/GPi pathway, and the late excitation by the cortico-striato-GPe-STN-GPe/GPi pathway.[12,13] We assume that the response components observed in the present human study were derived from the same pathways. However, a major response pattern in human patients was a monophasic inhibition. Such a pattern difference may be ascribed to the stimulus methods. Although stimulating wire electrodes were implanted inside the cortex of animals, disc electrodes on the cortical surface in this study may less effectively stimulate cortico-STN neurons, which are located in the deeper layer than corticostriatal neurons. The latencies of response components in this study (Table 2) were two times longer than those in monkeys[10–13] and three times longer than those in rodents.[14–16] These latency differences may be ascribed to the following reasons: (1) larger size of the human brain; (2) surface electrodes in this study may stimulate cortical neurons indirectly through afferent fibers or apical dendrites, whereas wire electrodes in animal studies may stimulate directly and instantly somata and axons; (3) pathological changes in PD.

Somatotopic Representations in the GPe/GPi

The somatotopic representations in the GPe/GPi have been repeatedly studied by movement-related activity during task performance, somatosensory inputs from muscles and joints, responses evoked by cortical stimulation and anatomical methods in nonhuman primates.[11,17,18] In the caudal part of the GPe/GPi, the orofacial area is represented in the most ventral part, and the lower limb area is found in the dorsal part. The upper limb area is located in between. The similar somatotopic representations were also reported in humans during stereotactic surgery.[19] The upper limb area occupies a large region in the GPe/GPi and is a good target to search during surgery. In this study, we have succeeded in identifying the upper limb area in the GPe/GPi by neuronal responses evoked by MI-stimulation, as well as by somatosensory inputs.

Targeting the Motor Territories of the GPe/GPi

The motor territory of the GPi is usually identified during stereotactic surgery by conventional electrophysiological methods, such as observing responses to passive/active movements.[8,9] The method introduced in this study, examining the unitary responses induced by MI-stimulation, can also identify the motor territories of the GPe/GPi. Some neurons that responded to MI-stimulation did not show somatosensory responses

probably because stimulus conditions were not optimal, especially during surgery. The effective cathodal contacts tended to be located close to the responding neurons. On the other hand, this method is more complex and time-consuming than the conventional ones, and thus, it is more appropriate in special cases, such as in patients under sedation, with considerable damage or with previous lesions in the basal ganglia; when spontaneous firing patterns or somatosensory responses are less obvious; and in cases aimed for research purposes.

Pathophysiology of Movement Disorders

There are many reports on GPe/GPi activity in PD patients and parkinsonian monkeys.[20–23] Decreased activity along the striato-GPi direct pathway and increased activity along the striato-GPe indirect pathway have been considered to cause increased GPi activity and finally interfere with disinhibitory process of releasing appropriate movements in PD.[24] Although not significant, firing rate of GPi neurons was higher than that of GPe neurons in this study (Table 2), supporting the firing rate theory. However, this study failed to show difference in durations of inhibitions between GPe and GPi neurons. Contrary to the firing rate theory, recent studies have focused on abnormal burst and oscillatory activity in the GPe/GPi underlying the PD pathophysiology.[25] Most neurons in this study showed burst or oscillatory burst activity.

On the other hand, reports on GPe/GPi activity in CD patients are limited.[26] The GPi firing rate in CD patients was lower than that in PD patients. GPi neurons fired in a more irregular pattern with more frequent and longer pauses in CD patients compared with PD patients. GPe/GPi activity in generalized dystonia decreased and became bursty.[27,28] The present data showed decreased GPe/GPi activity in the CD patient compared with the PD patients, and burst and oscillatory burst activity, agreeing with the previous reports.[26] Moreover, MI-stimulation induced a long-lasting inhibition in the GPe/GPi (Fig. 1, A5 and A6), suggesting increased activity along the cortico-striato-GPe/GPi pathway. Recently, the mouse model of dystonia also showed a long-lasting inhibition evoked by cortical stimulation in the GPe/GPi,[16] which is very similar to that observed in this study. Thus, increased activity along both the cortico-striato-GPi direct and cortico-striato-GPe indirect pathways is considered to be a fundamental change in dystonia. Reduced GPi output should disinhibit thalamic and cortical activity, resulting in involuntary movements observed in dystonia.

References

1. Rodriguez-Oroz MC, Obeso JA, Lang AE, et al. Bilateral deep brain stimulation in Parkinson's disease: a multicentre study with 4 years follow-up. Brain 2005;128:2240–2249.
2. Volkmann J, Allert N, Voges J, Sturm V, Schnitzler A, Freund HJ. Long-term results of bilateral pallidal stimulation in Parkinson's disease. Ann Neurol 2004;55:871–875.
3. Peppe A, Pierantozzi M, Altibrandi MG, et al. Bilateral GPi DBS is useful to reduce abnormal involuntary movements in advanced Parkinson's disease patients, but its action is related to modality and site of stimulation. Eur J Neurol 2001;8:579–586.
4. Starr PA, Turner RS, Rau G, et al. Microelectrode-guided implantation of deep brain stimulators into the globus pallidus internus for dystonia: techniques, electrode locations, and outcomes. J Neurosurg 2006;104:488–501.
5. Lombardi WJ, Gross RE, Trepanier LL, Lang AE, Lozano AM, Saint-Cyr JA. Relationship of lesion location to cognitive outcome following microelectrode-guided pallidotomy for Parkinson's disease: support for the existence of cognitive circuits in the human pallidum. Brain 2000;123:746–758.
6. Vitek JL, Bakay RA, Hashimoto T, et al. Microelectrode-guided pallidotomy: technical approach and its application in medically intractable Parkinson's disease. J Neurosurg 1998;88:1027–1043.
7. Yelnik J, Damier P, Bejjani BP, et al. Functional mapping of the human globus pallidus: contrasting effect of stimulation in the internal and external pallidum in Parkinson's disease. Neuroscience 2000;101:77–87.
8. Hutchison WD, Lozano AM.Microelectrode recordings in movement disorder surgery. In: Lozano AM, editor. Movement disorder surgery. Basel: Karger; 2000. p 103–117. (Progress in Neurological Surgery; Vol. 15).
9. Kaplitt MG, Hutchison WD, Lozano AM.Target localization in movement disorders surgery. In: Tarsy D, Vitek JL, Lozano AM, editors. Surgical treatment of Parkinson's disease and other movement disorders. Totowa: Humana Press; 2003. p 87–98.
10. Nambu A, Tokuno H, Hamada I, et al. Excitatory cortical inputs to pallidal neurons via the subthalamic nucleus in the monkey. J Neurophysiol 2000;84:289–300.
11. Yoshida S, Nambu A, Jinnai K. The distribution of the globus pallidus neurons with input from various cortical areas in the monkeys. Brain Res 1993;611:170–174.
12. Kita H, Nambu A, Kaneda K, Tachibana Y, Takada M. Role of ionotropic glutamatergic and GABAergic inputs on the firing activity of neurons in the external pallidum in awake monkeys. J Neurophysiol 2004;92:3069–3084.
13. Tachibana Y, Kita H, Chiken S, Takada M, Nambu A. Motor cortical control of internal pallidal activity through glutamatergic and GABAergic inputs in awake monkeys. Eur J Neurosci 2008; 27:238–253.
14. Maurice N, Deniau JM, Glowinski J, Thierry AM. Relationships between the prefrontal cortex and the basal ganglia in the rat: physiology of the cortico-nigral circuits. J Neurosci 1999;19: 4674–4681.
15. Ryan LJ, Clark KB. The role of the subthalamic nucleus in the response of globus pallidus neurons to stimulation of the prelimbic and agranular frontal cortices in rats. Exp Brain Res 1991;86: 641–651.
16. Chiken S, Shashidharan P, Nambu A. Cortically evoked long-lasting inhibition of pallidal neurons in a transgenic mouse model of dystonia. J Neurosci 2008;28:13967–13977.
17. DeLong MR, Crutcher MD, Georgopoulos AP. Primate globus pallidus and subthalamic nucleus: functional organization. J Neurophysiol 1985;53:530–543.
18. Strick PL, Dum RP, Picard N. Macro-organization of the circuits connecting the basal ganglia with the cortical motor areas. In: Houck JC, Davis JL, Beiser DG, editors. Models of information processing in the basal ganglia. Cambridge: MIT Press; 1995. p 117–130.
19. Guridi J, Gorospe A, Ramos E, Linazasoro G, Rodriguez MC, Obeso JA. Stereotactic targeting of the globus pallidus internus in Parkinson's disease: imaging versus electrophysiological mapping. Neurosurgery 1999;45:278–287; discussion 287–279.
20. Bergman H, Wichmann T, Karmon B, DeLong MR. The primate subthalamic nucleus. II. Neuronal activity in the MPTP model of parkinsonism. J Neurophysiol 1994;72:507–520.
21. Raz A, Vaadia E, Bergman H. Firing patterns and correlations of spontaneous discharge of pallidal neurons in the normal and the tremulous 1-methyl-4-phenyl-1,2,3,6-tetrahydropyridine vervet model of parkinsonism. J Neurosci 2000;20:8559–8571.

22. Hutchison WD, Levy R, Dostrovsky JO, Lozano AM, Lang AE. Effects of apomorphine on globus pallidus neurons in parkinsonian patients. Ann Neurol 1997;42:767–775.

23. Magnin M, Morel A, Jeanmonod D. Single-unit analysis of the pallidum, thalamus and subthalamic nucleus in parkinsonian patients. Neuroscience 2000;96:549–564.

24. DeLong MR. Primate models of movement disorders of basal ganglia origin. Trends Neurosci 1990;13:281–285.

25. Brown P. Abnormal oscillatory synchronisation in the motor system leads to impaired movement. Curr Opin Neurobiol 2007;17:656–664.

26. Tang JK, Moro E, Mahant N, et al. Neuronal firing rates and patterns in the globus pallidus internus of patients with cervical dystonia differ from those with Parkinson's disease. J Neurophysiol 2007;98:720–729.

27. Vitek JL, Chockkan V, Zhang JY, et al. Neuronal activity in the basal ganglia in patients with generalized dystonia and hemiballismus. Ann Neurol 1999;46:22–35.

28. Starr PA, Rau GM, Davis V, et al. Spontaneous pallidal neuronal activity in human dystonia: comparison with Parkinson's disease and normal macaque. J Neurophysiol 2005;93:3165–3176.

EUROPEAN JOURNAL OF NEUROSCIENCE

European Journal of Neuroscience, Vol. 34, pp. 1470–1484, 2011 doi:10.1111/j.1460-9568.2011.07865.x

NEUROSYSTEMS

Subthalamo-pallidal interactions underlying parkinsonian neuronal oscillations in the primate basal ganglia

Yoshihisa Tachibana,[1,2] Hirokazu Iwamuro,[1] Hitoshi Kita,[3] Masahiko Takada[4] and Atsushi Nambu[1,2]
[1]Division of System Neurophysiology, National Institute for Physiological Sciences, Okazaki, Aichi, Japan
[2]Department of Physiological Sciences, The Graduate University for Advanced Studies, Okazaki, Aichi, Japan
[3]Department of Anatomy and Neurobiology, College of Medicine, University of Tennessee Health Science Center, Memphis, TN, USA
[4]Systems Neuroscience Section, Primate Research Institute, Kyoto University, Inuyama, Aichi, Japan

Keywords: GABA, globus pallidus, glutamate, parkinsonian monkeys, subthalamic nucleus

Abstract

Parkinson's disease is characterized by degeneration of nigral dopaminergic neurons, leading to a wide variety of psychomotor dysfunctions. Accumulated evidence suggests that abnormally synchronized oscillations in the basal ganglia contribute to the expression of parkinsonian motor symptoms. However, the mechanism that generates abnormal oscillations in a dopamine-depleted state remains poorly understood. We addressed this question by examining basal ganglia neuronal activity in two 1-methyl-4-phenyl-1,2,3,6-tetrahydropyridine-treated parkinsonian monkeys. We found that systemic administration of L-3,4-dihydroxyphenylalanine (L-DOPA; dopamine precursor) decreased abnormal neuronal oscillations (8–15 Hz) in the internal segment of the globus pallidus (GPi) and the subthalamic nucleus (STN) during the ON state when parkinsonian signs were alleviated and during L-DOPA-induced dyskinesia. GPi oscillations and parkinsonian signs were suppressed by silencing of the STN with infusion of muscimol ($GABA_A$ receptor agonist). Intrapallidal microinjection of a mixture of 3-(2-carboxypiperazin-4-yl)-propyl-1-phosphonic acid (CPP; *N*-methyl-D-aspartate receptor antagonist) and 1,2,3,4-tetrahydro-6-nitro-2,3-dioxo-benzo[*f*]quinoxaline-7-sulfonamide (NBQX; AMPA/kainate receptor antagonist) also decreased the oscillations in the GPi and the external segment of the globus pallidus (GPe). Neuronal oscillations in the STN were suppressed after intrasubthalamic microinjection of CPP/NBQX to block glutamatergic afferents of the STN. The STN oscillations were further reduced by muscimol inactivation of the GPe to block GABAergic inputs from the GPe. These results suggest that, in the dopamine-depleted state, glutamatergic inputs to the STN and reciprocal GPe–STN interconnections are both important for the generation and amplification of the oscillatory activity of STN neurons, which is subsequently transmitted to the GPi, thus contributing to the symptomatic expression of Parkinson's disease.

Introduction

Degeneration of nigral dopaminergic neurons is associated with motor symptoms of Parkinson's disease (PD), which include bradykinesia, rigidity, and tremor. Changes in the firing rates of basal ganglia (BG) neurons are thought to induce the PD symptoms (Albin *et al.*, 1989; DeLong, 1990). Contrary to the rate-based theory, the pathophysiology of PD is often correlated with abnormal burst firing and oscillatory activity in the BG (Filion, 1979; Wichmann *et al.*, 1994; for reviews, see Boraud *et al.*, 2002; Brown, 2003; Gatev *et al.*, 2006; Rivlin-Etzion *et al.*, 2006a; Hammond *et al.*, 2007). Single/multi-unit activity and local field potentials (LFPs) recorded from parkinsonian animals and patients have shown that oscillatory activity and neuronal synchronization in the globus pallidus and the subthalamic nucleus (STN) include two major frequency bands: the 'tremor-related' 3–8-Hz band and the higher 8–30-Hz band (Bergman *et al.*, 1994; Levy *et al.*, 2000; Brown *et al.*, 2001). However, the mechanisms regulating the abnormal BG oscillations remain unknown.

The first goal of the present study was to examine whether parkinsonian BG oscillations might depend on dopaminergic inputs. Dopamine therapy can ameliorate parkinsonian signs and, at least partly, reverse the abnormal firing pattern of spike trains (Boraud *et al.*, 1998; Levy *et al.*, 2001a, 2002; Heimer *et al.*, 2006; Lafreniere-Roula *et al.*, 2010) and neuronal synchronization observed in LFPs (Brown *et al.*, 2001; Cassidy *et al.*, 2002; Priori *et al.*, 2004) in the BG. However, little is known about systemic dopamine-dependent changes in the firing properties of neurons of the internal segment of the globus pallidus (GPi), external segment of the globus pallidus (GPe) and STN in the same parkinsonian subject. Thus, we tested the effects of intravenous L-3,4-dihydroxyphenylalanine (L-DOPA) injection on BG neuronal activity in 1-methyl-4-phenyl-1,2,3,6-tetrahydropyridine (MPTP)-treated monkeys (Fig. 1A). The second

Correspondence: Atsushi Nambu and Yoshihisa Tachibana, [1]Division of System Neurophysiology, as above.
E-mails: nambu@nips.ac.jp and banao@nips.ac.jp

Received 20 May 2011, revised 3 August 2011, accepted 8 August 2011

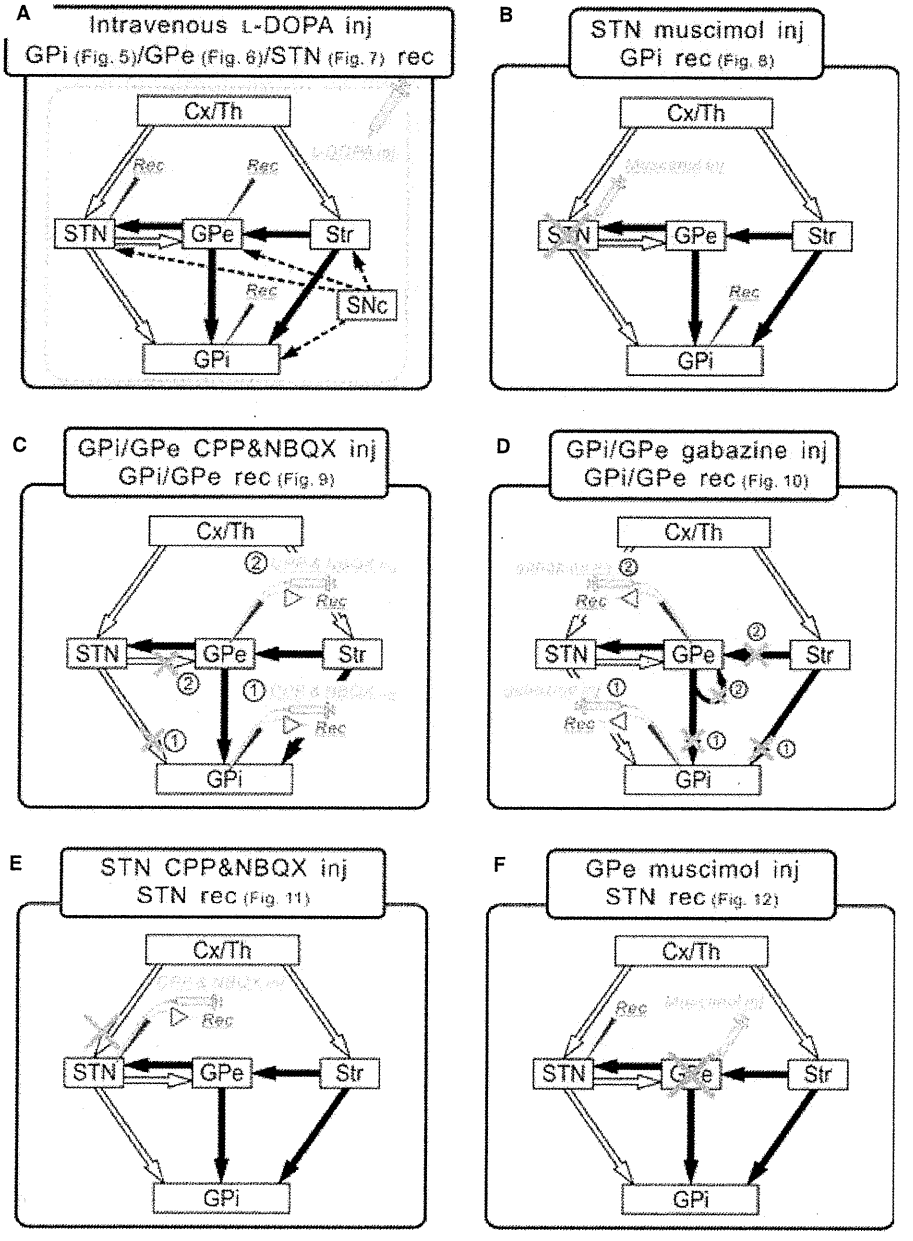

FIG. 1. Schematic diagrams of experiments in parkinsonian monkeys. Anatomical connections within cortico-BG circuits are shown. Open, filled and broken arrows represent glutamatergic, GABAergic and dopaminergic projections, respectively. The striatum (Str) and STN are two major input nuclei of the BG. Inputs from the cortex (Cx) and the thalamus (Th) enter the two nuclei and finally reach the GPi, an output nucleus of the BG. The GPe is positioned as an intermediate relay system, which is reciprocally interconnected with the STN. Dopaminergic projections from the substantia nigra pars compacta (SNc) are widely distributed in the BG. The following experiments were performed to examine the mechanisms regulating abnormal neuronal oscillations in the BG. (A) Single-unit recording of a GPi, a GPe or an STN neuron with intravenous injection of the dopamine precursor L-DOPA to restore dopamine levels (see Fig. 5 for GPi, Fig. 6 for GPe, and Fig. 7 for STN). (B) Recording from a GPi neuron with muscimol injection into the STN to block subthalamic inputs to the GPi (see Fig. 8). (C) Recording from a GPi (1) or a GPe (2) neuron with intrapallidal microinjection of the ionotropic glutamate receptor antagonists CPP and NBQX to block glutamatergic inputs to the GPi or GPe (see Fig. 9A–G for GPi and Fig. 9H–N for GPe). (D) Recording from a GPi (1) or a GPe (2) neuron with intrapallidal microinjection of the ionotropic GABA receptor antagonist gabazine to block GABAergic inputs to the GPi or GPe (see Fig. 10). Gabazine injection into the GPi blocked GABAergic inputs from the Str and GPe, and injection into the GPe blocked the inputs from the Str and GPe axon collaterals. (E) Recording from an STN neuron with intrasubthalamic microinjection of CPP and NBQX to block glutamatergic inputs to the STN (see Fig. 11). (F) Recording from an STN neuron with muscimol injection into the GPe to block GPe-derived GABAergic inputs (see Fig. 12).

goal of our study was to clarify the origin of GPi/GPe oscillations. Recordings of LFPs from PD patients show elevated levels of coherence between the STN and GPi (Brown *et al.*, 2001). The STN consists of glutamatergic projection neurons, and strongly influences GPi/GPe activity. To provide direct evidence that STN oscillations may drive oscillations in the GPi/GPe, we performed single-unit GPi/GPe recordings while STN glutamatergic inputs were blocked (Fig. 1B and C). Finally, the origin of STN oscillations was also investigated. Glutamatergic inputs from the cerebral cortex and the thalamus may drive STN oscillations (Magill *et al.*, 2000, 2001;

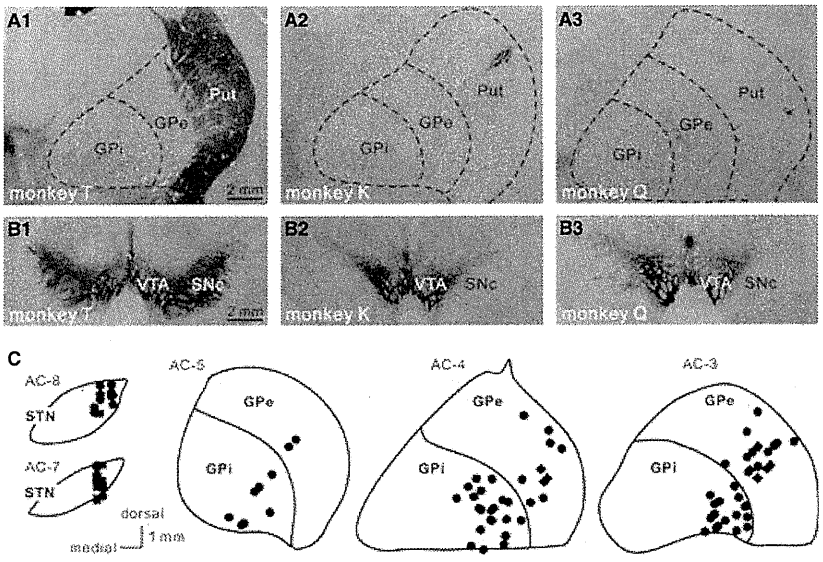

FIG. 2. TH immunoreactivity in the BG sampled from normal and MPTP-treated monkeys, and sites of unit recordings and drug injections in the STN and GPi/GPe. (A and B) Photomicrographs showing TH immunoreactivity in the putamen (Put; A1–A3) and the midbrain tegmentum (B1–B3). Sections in A1 and B1 are from a normal monkey (monkey T), and sections in A2, A3, B2 and B3 are from MPTP-treated monkeys (monkeys K and Q). As compared with the control (A1 and B1), marked reductions in TH immunoreactivity were observed in the Put (A2 and A3) and the ventral tier of the substantia nigra pars compacta (SNc) (B2 and B3) of the MPTP-treated monkeys. Note that numbers of TH-positive cells still remain in the dorsal tier of the SNc and the ventral tegmental area (VTA). The sections shown in A2 and A3 and the right side of the sections shown in B2 and B3 represent the sides ipsilateral to the carotid injections of MPTP and electrophysiological recordings. (C) Sites of unit recordings and drug injections in the STN and GPi/GPe are reconstructed from two MPTP-treated monkeys, and superimposed on representative coronal sections. Levels of the sections are indicated as distances (mm) from the caudal end of the anterior commissure (AC). Filled circles and squares represent the recording and injection sites, respectively. These sites are located within the motor territories of the STN and GPi/GPe (Nambu *et al.*, 2000; Tachibana *et al.*, 2008).

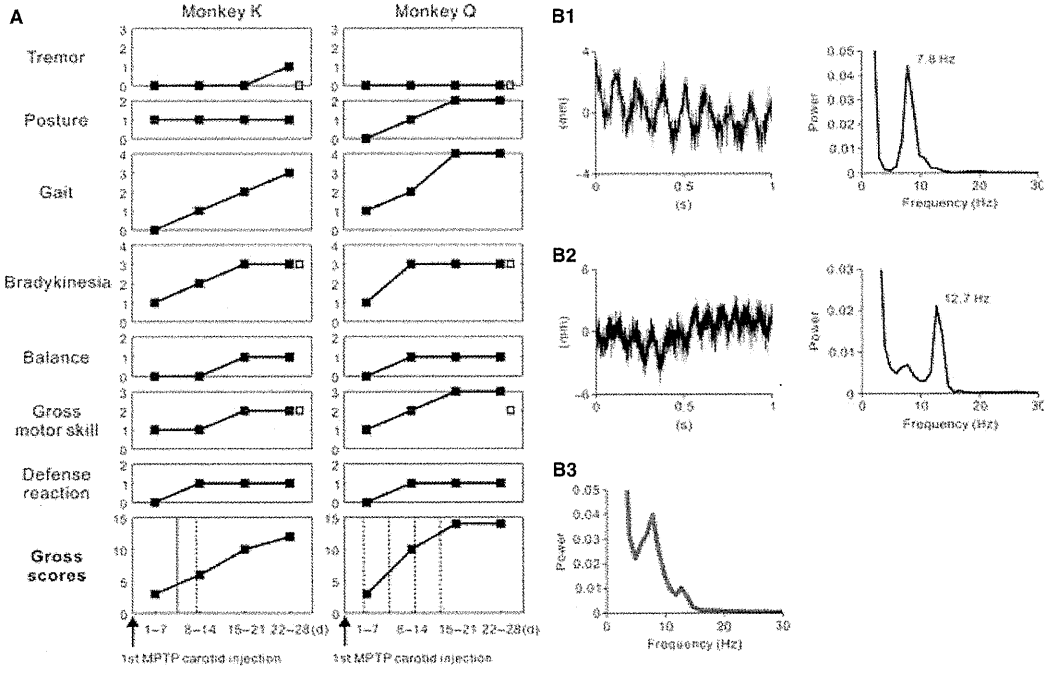

FIG. 3. Parkinsonian motor signs. (A) Parkinsonian rating scale. With the monkey parkinsonian rating scale of Smith *et al.* (1993), a variety of motor signs were evaluated (see also Supporting Information Data S1). Partial and gross motor scores are plotted along the time course (days) after the first carotid injection of MPTP. Filled and open squares represent the scores on the contralateral or ipsilateral side to the carotid injection, respectively. The partial scores on the ipsilateral side were estimated only at the behaviorally stable stage. The solid vertical line for the gross scores represents the timing of the second MPTP carotid injection. The broken vertical lines represent the timings of additional intravenous MPTP injections. (B) Resting tremor in monkey K. Small forearm movements were detected with a laser displacement sensor (LK-500; sampling rate, 1 kHz; Keyence, Osaka, Japan). (B1 and B2) Two representative raw data of a 7.8-Hz dominant (B1) and a 12.7-Hz dominant (B2) tremor episode are shown in the left panels. The power spectra of each tremor episode are shown in the right panels. Power spectrum analyses were performed with 5-s raw data with a non-overlapping Hann window of 1024 bins, yielding a spectral resolution of 1 Hz. (B3) Averaged power spectrum from 41 tremor episodes, exhibiting two peaks at 7.8 and 12.7 Hz.

TABLE 1. Electrophysiological properties of GPe, GPi and STN neurons recorded before and after MPTP injections. (A) Monkey K. (B) Monkey Q

	GPe		GPi		STN	
	Normal (n = 51)	MPTP (n = 41)	Normal (n = 52)	MPTP (n = 32)	Normal (n = 47)	MPTP (n = 30)
(A)						
Firing rate (Hz)	64.7 ± 27.5	44.7 ± 23.1**	70.3 ± 26.0	73.0 ± 30.4	20.8 ± 11.4	30.7 ± 13.0***
Percentage of spikes in bursts (%)	14.0 ± 12.8	23.1 ± 17.2**	10.6 ± 11.3	22.7 ± 17.4***	24.4 ± 12.9	36.2 ± 12.0***
Mean 'surprise value'	4.30 ± 1.13	4.99 ± 2.11	4.32 ± 0.89	5.22 ± 2.33**	5.55 ± 1.50	5.71 ± 1.14
Number of 3–8-Hz oscillatory cells (%)	9/51 (17.6)	4/41 (9.8)	25/52 (48.1)	12/32 (37.5)	4/47 (8.5)	4/30 (6.7)
Mean 3–8-Hz power	1.09 ± 0.14	1.06 ± 0.12	1.26 ± 0.30	1.22 ± 0.43	1.04 ± 0.10	1.10 ± 0.13
Number of 8–15-Hz oscillatory cells (%)	0/51 (0.0)	4/41 (9.8)*	0/52 (0.0)	23/32 (71.9)***	4/47 (8.5)	10/30 (33.3)**
Mean frequency with maximum power at 8–15 Hz (Hz)	NA	12.6 ± 1.3 (n = 4)	NA	12.7 ± 1.3 (n = 23)	11.0 ± 2.2 (n = 4)	13.5 ± 0.6 (n = 10)
Mean 8–15-Hz power	0.82 ± 0.10	0.95 ± 0.13***	0.87 ± 0.10	1.31 ± 0.29***	0.97 ± 0.10	1.10 ± 0.13***
	Normal (n = 54)	MPTP (n = 40)	Normal (n = 75)	MPTP (n = 68)	Normal (n = 44)	MPTP (n = 25)
(B)						
Firing rate (Hz)	65.6 ± 24.2	37.6 ± 21.6***	64.8 ± 22.9	58.4 ± 23.9	18.6 ± 7.6	23.9 ± 8.0*
Percentage of spikes in bursts (%)	14.7 ± 14.4	41.1 ± 24.1***	7.0 ± 7.0	20.2 ± 15.0***	32.6 ± 16.4	40.9 ± 14.9*
Mean 'surprise value'	4.53 ± 1.25	6.73 ± 3.15***	4.13 ± 0.97	4.98 ± 1.40**	5.36 ± 1.24	6.14 ± 1.72*
Number of 3–8-Hz oscillatory cells (%)	17/54 (31.5)	11/40 (27.5)	28/75 (37.3)	28/68 (41.2)	1/44 (2.2)	4/25 (16.0)*
Mean 3–8-Hz power	1.13 ± 0.24	1.18 ± 0.17	1.15 ± 0.25	1.18 ± 0.28	1.00 ± 0.19	1.13 ± 0.20**
Number of 8–15-Hz oscillatory cells (%)	0/54 (0.0)	4/40 (10.0)*	0/75 (0.0)	23/68 (33.8)***	2/44 (4.5)	6/25 (24.0)*
Mean frequency with maximum power at 8–15 Hz (Hz)	NA	10.7 ± 0.8 (n = 4)	NA	11.4 ± 1.0 (n = 23)	11.7 ± 3.5 (n = 2)	10.7 ± 1.9 (n = 6)
Mean 8–15-Hz power	0.79 ± 0.13	0.87 ± 0.13*	0.76 ± 0.11	1.05 ± 0.36***	0.94 ± 0.17	1.02 ± 0.15*

Firing properties of GPe, GPi and STN neurons are represented as mean ± SD. Mann–Whitney U-tests were performed between normal and parkinsonian states. The proportions of oscillatory cells were compared by use of Fisher's exact tests. NA, data not available. Significance levels are as follows: *$P < 0.05$, **$P < 0.01$, ***$P < 0.001$.

Williams *et al.*, 2002; Sharott *et al.*, 2005; Mallet *et al.*, 2008b). It has also been demonstrated by Baufreton *et al.* (2005a) that excitation together with feedback GABAergic inhibition from the GPe is sufficient to generate highly synchronous activity (15–30 Hz) of STN neurons *in vitro*. However, it is unknown how the glutamatergic and pallidal GABAergic inputs contribute to STN oscillations. To address this issue, we examined STN activity during blockade of the two synaptic inputs (Fig. 1E and F). We found that, in the dopamine-depleted state, the oscillatory activity of STN neurons is generated by both the glutamatergic and the GPe-derived GABAergic inputs, and finally transmitted to the GPi.

Materials and methods

Surgical procedures

Two male monkeys (*Macaca cyclopis*, monkey K, and *Macaca mulatta*, monkey Q) weighing 3.5–5.0 kg were used as subjects in this study. The experimental protocols were approved by the Institutional Animal Care and Use Committee of National Institutes of Natural Sciences, and all experiments were conducted according to the guidelines of the National Institutes of Health *Guide for the Care and Use of Laboratory Animals*.

Prior to the experiments, each monkey was trained to sit quietly in a monkey chair. Under general anesthesia with intramuscular ketamine hydrochloride (10 mg/kg body weight) and intravenous sodium pentobarbital (25 mg/kg), the monkeys underwent a surgical procedure for head fixation and extracellular recordings of GPi/GPe and STN neurons, as reported previously (Nambu *et al.*, 2000; Tachibana *et al.*, 2008). Magnetic resonance imaging (3T Allegra; Siemens, Erlangen, Germany) scans were performed to estimate stereotaxic coordinates of the brain structures. Recordings of neuronal activity in the GPi/GPe and STN under normal conditions were initiated 2 weeks after the initial surgery.

Electrophysiological recording

During the recording sessions, each monkey was in an awake state and seated in the monkey chair with his head restrained. Single-unit recordings of GPi/GPe and STN neurons were performed with a glass-coated Elgiloy microelectrode (0.8–1.2 MΩ at 1 kHz for GPi/GPe; 1.5–2.0 MΩ for STN). The electrode was inserted obliquely (45° from vertical in the frontal plane) into the GPi/GPe or vertically into the STN with a hydraulic microdrive. The unitary activity recorded from the microelectrode was amplified (×8000), filtered (100 Hz to 2 kHz), converted into digital data with a window discriminator, and sampled at 2 kHz with a computer. In this study, we examined neuronal populations sampled from the motor territories (forelimb and orofacial regions) of the GPi/GPe and STN (Nambu *et al.*, 2000; Tachibana *et al.*, 2008); the recording sites were located in the lateral parts of individual structures at their middle to caudal levels (Fig. 2C). The subdivisions of the pallidum (i.e. GPe and GPi) were determined by the depth of recording electrodes, firing patterns and decreased electrical signals in the lamina between the GPe and GPi (Nambu *et al.*, 2000). The monkey's arousal level was visually monitored and maintained during recording sessions. Only stable and well-isolated neurons were included in the present data.

MPTP injections

After the recordings of GPi/GPe and STN neurons in the normal state, systemic administration of MPTP (Sigma, St Louis, MO, USA) was performed under the same general anesthesia as described above (Kaneda *et al.*, 2005). The MPTP injection (1.2 mg/kg) unilateral to the recording side was made through the common carotid artery with the external carotid artery clamped (Fig. 2A and B). With the monkey parkinsonian rating scale (Smith *et al.*, 1993; see also Supporting Information Data S1), motor signs were quantitatively evaluated (the maximum parkinsonian score was 20; that is, more serious parkinsonian stages were indicated by higher scores; Fig. 3A). To make moderate to severe parkinsonian models, monkeys received an additional carotid artery injection (1.0 mg/kg, 1 week after the first injection) and/or intravenous injections through the great saphenous vein (0.3 mg/kg every 4 days, 3 days after the last carotid injection). Monkey K received carotid injections twice (1.2 and 1.0 mg/kg) and intravenous injection once, and monkey Q received carotid injection once and intravenous injection four times. The total doses of MPTP were 2.5 mg/kg for monkey K and 2.4 mg/kg for monkey Q. Unit recordings of BG neurons in the parkinsonian state was started after the parkinsonian scores became stable, that is, 2 weeks (monkey K) and 3 weeks (monkey Q) after the final MPTP injection.

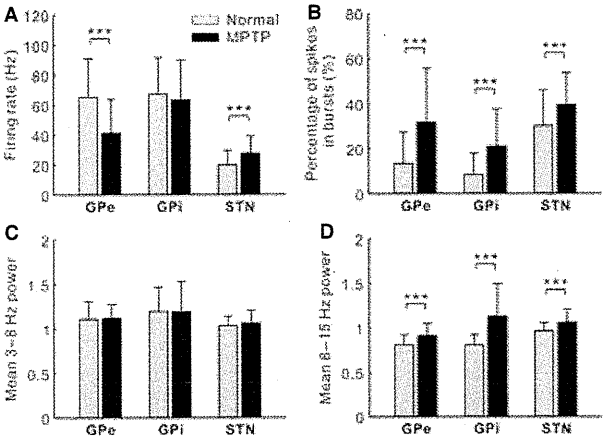

FIG. 4. Comparison of electrophysiological properties of BG neurons in normal and parkinsonian monkeys. (A) Spontaneous firing rates. Gray and black columns show the average firing rates in normal and MPTP-treated monkeys, respectively. Data are given as mean ± SD. The same conventions are used in B–D. The GPe firing rate was significantly decreased after MPTP treatment, whereas the STN firing rate was significantly increased. (B) Percentage of spikes in bursts. The bursts were detected with the 'Poisson surprise' algorithm. The burst strength was increased in all three structures. (C) Averaged power of 3–8-Hz oscillatory activity. Oscillatory activity was calculated on the basis of the algorithm of Rivlin-Etzion *et al.* (2006b). There were no changes in 3–8-Hz oscillatory activity. (D) Averaged power of 8–15-Hz oscillatory activity. Significant increases in 8–15-Hz oscillatory power were detected in all three structures. The pooled data from two monkeys were the same as those for the neuronal populations in Table 1. ***$P < 0.001$.

L-DOPA treatments

We investigated the effects of systemic dopamine administration on the neuronal activity of GPi/GPe and STN neurons in the parkinsonian state. After the control recordings of GPi/GPe and STN neurons, 3.5 mg/kg (monkey K) or 2.5 mg/kg (monkey Q) L-DOPA (DOPASTON, a dopamine precursor; Sankyo, Tokyo, Japan) was manually injected into the great saphenous vein at a low rate, and this was followed by the infusion of electrolyte fluid. To verify the contingency between the L-DOPA-induced behavioral effects and the activity changes in BG neurons, we avoided using Carbidopa, which could prevent the conversion of L-DOPA to dopamine peripherally and delay

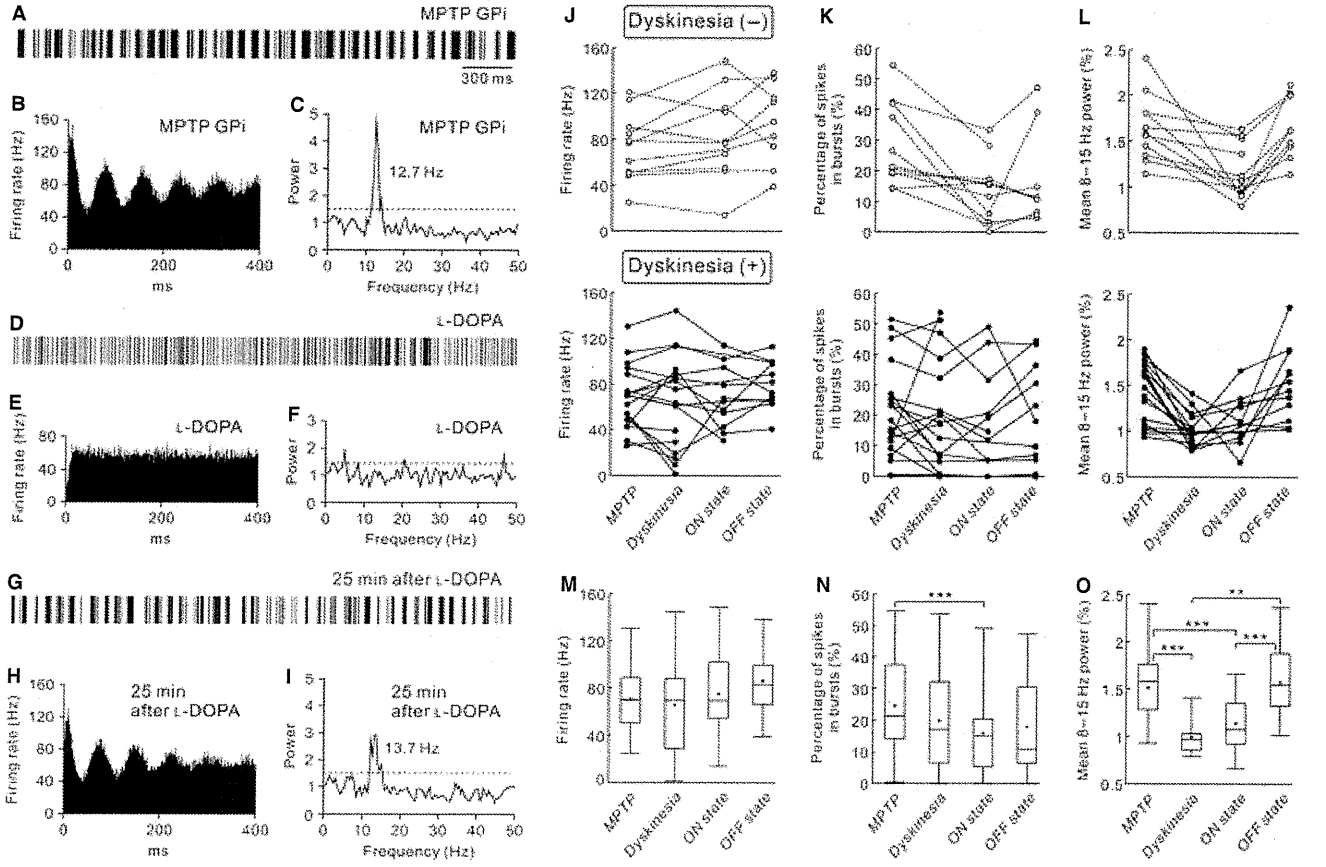

FIG. 5. L-DOPA effects on dopamine-depleted GPi neurons. (A, D and G) Representative 3-s digitized spikes from a 50-s spike train before and after intravenous L-DOPA injection. (B, E and H) Autocorrelograms calculated from the same spike train (bin width, 0.5 ms). (C, F and I) Power spectra of the same spike trains, compensated by the algorithm of Rivlin-Etzion *et al.* (2006b). Gray dashed lines represent a confidence level of $P = 0.01$. Peak frequency in the range of 8–15 Hz is also shown. A GPi neuron showed 8–15-Hz oscillations in the parkinsonian state (A–C). An intravenous L-DOPA injection reduced the 8–15-Hz oscillatory activity in the GPi (D–F), with an improvement in parkinsonian motor signs (ON state). Twenty-five minutes after the L-DOPA injection, the oscillatory activity resumed (G–I). At this time, recuperation from the parkinsonism was not observed (OFF state). (J–L) Changes in the spontaneous firing rate (J), the burst strength (K) and the mean 8–15-Hz power spectrum of spike trains (L) after the L-DOPA injections. The upper rows show the neurons recorded without dyskinesia. The lower rows show the neurons recorded with the development of dyskinesia. Data are plotted along the behavioral changes, and the data points from the same neuron are connected with lines. Owing to the excessive body movement of the monkeys, some GPi neurons were lost during neuronal recording. (M–O) Summaries of the L-DOPA effects on the firing rate (M), the burst strength (N) and the mean 8–15-Hz power (O) in 29 GPi neurons examined. In box plots, means are indicated as black dots. In this and subsequent figures, the repeated Wilcoxon signed-rank tests were performed to calculate statistically significant differences among pre-injection (labeled as MPTP) and post-injection (dyskinesia, ON state and OFF state) conditions. In the GPi neurons tested, the overall firing rate did not change throughout the injections. In contrast, the power of 8–15-Hz oscillations was significantly decreased from pre-injection states to dyskinetic states and to ON states. A significant decrease in the burst strength was also detected between pre-injection states and ON states. $^{**}P < 0.01$, $^{***}P < 0.001$.

the termination of the L-DOPA effects. An optimal dose of L-DOPA was determined so that the injection would reduce the gross parkinsonian scores by 5 or more. The L-DOPA effects on neuronal activity in the GPi/GPe and STN appeared within approximately 5 min. During this period, the L-DOPA greatly improved the motor symptoms of both monkeys, and eventually induced dyskinetic movements (dyskinetic state). The dyskinesia typically appeared as oral dyskinesia and/or forelimb dyskinesia, and sometimes spread to entire body parts. The excessive dyskinetic state usually ceased in 5–10 min and shifted to the ON state without dyskinesia, termed the 'ON state'. Approximately 30 min after the injection, the animals exhibited the original parkinsonism, termed the 'OFF state'. In some cases, the L-DOPA effects appeared without development of the dyskinetic state. The L-DOPA experiments were limited to two injections per recording day, and the interval between the injections was >2 h throughout the experiments. It should be noted that the electrophysiological data for the dopamine-depleted state in Table 1 were collected before the following receptor-related drug injection experiments (monkey K, including the neurons sampled at least 48 h after the last L-DOPA injection; monkey Q, including the neurons recorded only in the L-DOPA-naive state).

Unit recordings with local drug injection

We developed a microinjection method to examine the impacts of direct synaptic inputs (i.e. glutamatergic and GABAergic inputs) on the oscillatory activity of individual BG neurons. Unit recordings of GPi/GPe or STN neurons with local drug injection were performed with an electrode assembly consisting of a glass-coated Elgiloy microelectrode for unit recording and a silica tube for drug delivery, as described previously (Tachibana *et al.*, 2008). Through the silica tube, one of the following drugs was injected (0.03–0.05 μL/min; total, 0.1–0.2 μL): (i) a mixture of an *N*-methyl-D-aspartate receptor antagonist, 3-(2-carboxypiperazin-4-yl)-propyl-1-phosphonic acid (CPP) (1 mM; Sigma), and an AMPA/kainate

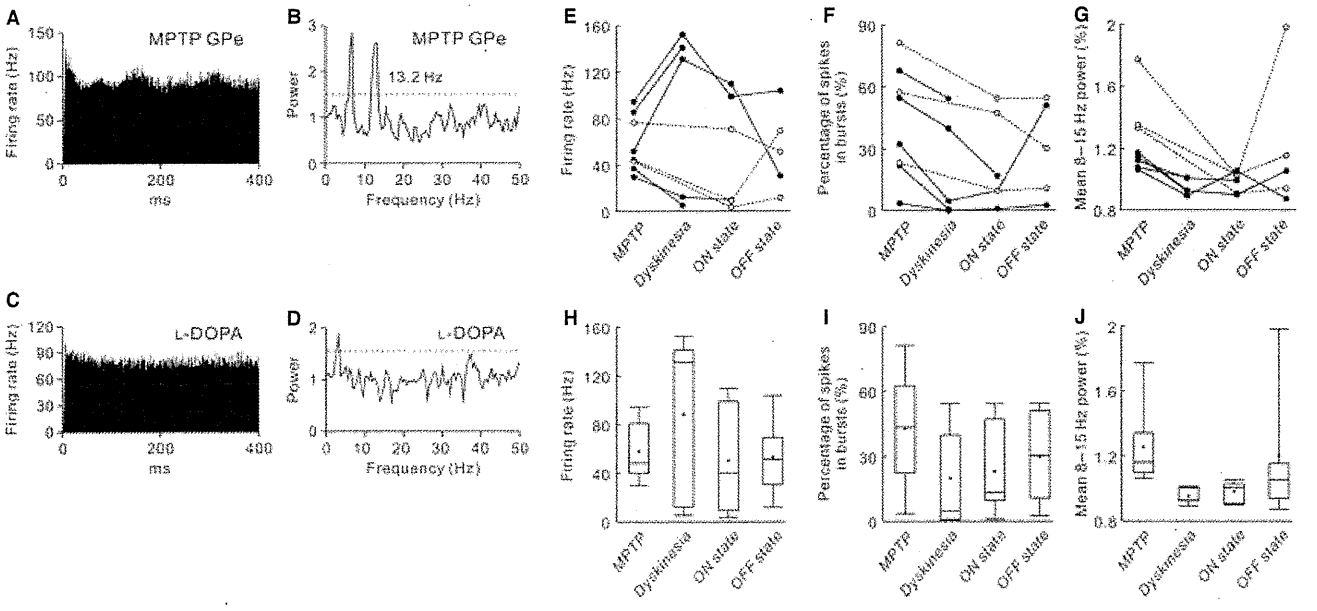

FIG. 6. L-DOPA effects on dopamine-depleted GPe neurons. (A and B) A GPe neuron showed 3–8-Hz and 8–15-Hz oscillations in the parkinsonian state. The conventions in this and the following figures are the same as in Fig. 5. (C and D) An intravenous L-DOPA injection suppressed both types of oscillation in the GPe neuron. (E–G) L-DOPA-induced changes in the spontaneous firing rate (E), the burst strength (F) and the mean 8–15-Hz power (G) of eight GPe neurons tested. Data from the neurons recorded without dyskinesia (open circles and broken lines) are superimposed on those from the neurons recorded with dyskinesia (filled circles and solid lines). (H–J) Summaries of the L-DOPA effects on the firing rate (H), the burst strength (I) and the mean 8–15-Hz power (J) in GPe neurons.

receptor antagonist, 1,2,3,4-tetrahydro-6-nitro-2,3-dioxo-benzo[*f*]quinoxaline-7-sulfonamide (NBQX) (1 mM; Sigma); and (ii) a $GABA_A$ receptor antagonist, gabazine (1 mM; Sigma). Injection sites were located at least 1 mm apart because the effective radius of the drugs was estimated to be approximately 1 mm (Tachibana *et al.*, 2008). This method limited unit recordings to a maximum of two GPi/GPe neurons or a single STN neuron per recording day.

Methods for inactivation of the STN or GPe were similar to the methods described elsewhere (Nambu *et al.*, 2000; Tachibana *et al.*, 2008). A Teflon-coated tungsten wire that was attached to the 31-gauge needle of a 10-μL Hamilton microsyringe, or the above electrode assembly, was inserted vertically into the STN or obliquely into the GPe with a hydraulic microdrive. A $GABA_A$ receptor agonist, muscimol (4.4 mM; 0.5–1.0 μL in the STN, 1–2 μL in the GPe; Sigma), was injected. Because the effect of muscimol on the target structure lasted for several hours, the inactivation of the STN or GPe was limited to a single injection per recording day.

Data analysis

Off-line data analysis was performed with MATLAB software (MathWorks, Natick, MA, USA). Spontaneous firing rates and patterns of the recorded neurons were analyzed by calculating the autocorrelograms (bin width, 0.5 ms) from 50 s of digitized recordings.

Bursts of GPi/GPe and STN neurons were detected on the basis of the 'Poisson surprise' algorithm, with a 'surprise value' of at least three and a number of spikes of at least three in a burst (Wichmann & Soares, 2006; see also Supporting Information Fig. S1). Briefly, the algorithm can calculate a probability that successive spikes occur in a given time window of a spike train, which is assumed to be Poisson-distributed with the same firing rate. If the successive spikes occur with a significantly low probability ('surprise'), the spikes are considered as a burst. The strength of bursts was estimated by the percentage of spikes in bursts (as compared with all spikes in the recording data), which has frequently been used in other studies (Levy *et al.*, 2001a; Wichmann & Soares, 2006). We also calculated the mean 'surprise value' of overall bursts detected by the algorithm. Oscillatory activity of GPi/GPe and STN neurons was estimated by spectral analysis of spike trains with a shuffling technique (Rivlin-Etzion *et al.*, 2006b). The method calculated the power spectral density (PSD) of spike trains based on Welch's method (Halliday *et al.*, 1995). The PSD calculation was performed with a non-overlapping Hann window with a length of 4096 bins. Because the sampling frequency of spike trains was 2 kHz, the frequency resolution was approximately 0.5 Hz. In the present study, the compensated PSD was obtained from the PSD of original spike trains divided by the mean PSD of locally (T = 175–225 ms) shuffled (n = 50) spike trains. The local shuffling method minimized the spectral distortion at lower frequencies caused by the refractory periods of neurons, and the effect of the neuronal firing rate on the PSD, thus enabling easy detection of periodic oscillatory phenomena in the recorded neurons. A confidence level ($P < 0.01$) of the compensated PSD was determined on the basis of the mean ± standard deviation (SD) of the PSD values in the range of 270–300 Hz, at which the PSD values were stable. Oscillatory cells were defined by determining whether their two consecutive PSD values within individual ranges of 3–8 and 8–15 Hz crossed the confidence level (Soares *et al.*, 2004). The power (strength) of 3–8- and 8–15-Hz oscillations was estimated by averaging the PSD values within the individual frequency bands, and termed 'mean 3–8-Hz power' and 'mean 8–15-Hz power', respectively. We also estimated the oscillatory activity in the range of 20–30 Hz in the same manner.

Histology

At the end of the final recordings, reference lesions were placed at several sites by passing a cathodal DC current of 20 μA through the